2023 Collegiate Wind Competition

OSU CYCLONE COWBOYS

SCHOOL OF
ELECTRICAL AND COMPUTER ENGINEERING
College of Engineering, Architecture and Technology

TURBINE DESIGN

Turbine Design Team:

Ben Marquis - Turbine Design Lead

Mary Urias - Testing

Maggie English - Testing

Wesley Dodson- Fabrication

John-Todd Wallace - Fabrication

Kaden Clemmer - Fabrication

Austin Elliot - Aero

Carinna Marling - CAD & Design

Ryan Lawson - CAD & Design

Peter Tkalsky - Electrical

Bret Vaughn - Electrical

Sahir Virani - Electrical

Mezyad Abusheeba - Anchor

Evelyn Baker - Anchor

Isaiah Cotton - Anchor

Madeline Duncan - Anchor

Faculty Advisor:

Nate Lannan - Electrical and Computer Engineer

Pete's Power Plant

Table of Contents

Executive Summary

Wind Energy is a leading energy source in Oklahoma, which is a large motivation for the Cyclone Cowboys, being from Oklahoma State University. With this being the first year OSU has competed in the competition, we have researched past projects and produced innovative plans to design a successful wind turbine. To conquer the task of building small scale offshore wind turbine, we have divided the turbine design into 3 sections: Mechanical Systems, Foundation, and Electrical Systems.

The Mechanical System includes the blades, a driveline, a braking system, a yaw system, and a nacelle for the turbine. We placed a large emphasis on blade design as blades are a crucial way to impact power generation. The blades were designed and optimized to produce a high RPM at a low cut in speed. Many iterations were fabricated using 3D printing with PLA and tested in a wind tunnel. Our final design features a TSR of 2.5 and is 3D printed with a carbon fiber reinforcement within the PLA to increase its strength. The driveline was designed in two parts: the female driveshaft and the male driveshaft. The male shaft is connected to the nosecone and enters the nacelle through a bearing. The male driveshaft then fits into the collar of the female driveshaft which is meant to support the brake system and mount to the motor. The braking system has two separate components. The first braking component is the brake force from the motor which modulates RPM through the load system. The second braking component is the mechanical disk, which completely stops the driveline when engaged by the servo.

Our foundation system is unique due to the shape we designed. A scooping configuration was designed for the anchor, which allows us to enforce the “no excavation rule” while adding durability to the turbine. It has a pole connected to a flat plate on top, which then concaves out on one side to insert the anchor into the sand. The anchor was made by welding a ferrous metal, scrap steel, and weighs 4 lbs.

The Electrical System is made up of a generator, a buck boost converter, and a load system. A three-phase brushless motor is used for our generator due to its high efficiency and low friction. A rectifier will be used to convert the AC output to DC. The motor has a kV rating between 100-200 which will increase efficiency while being able to stay under the 48 V constraint. The load system includes an autonomous resistor array, which determines the need to change its resistance value based on input power and voltage calculations through MOSFETs, LCPU, TCPU and UART communication.

Technical Design

Design Objective

Our goal throughout the competition has been to design, manufacture, and test a small-scale wind turbine that would mimic an offshore wind turbine. One of our main focuses was generating power while meeting all rules and constraints set by the CWC. Many factors were taken into consideration to reduce friction in the driveline subsystem, like the low-friction bearings used in the nacelle and the generator selected for final design. While generating the highest, most stable power possible, maintaining the durability and stability of the full assembly was imperative. Many subassembly and stress tests were performed to ensure the safety of our turbine using competition parameters.

Influence From Previous Teams

As a first-year team starting from a blank slate we looked through previous design reports and chose to focus on Wildcat Wind Power’s turbine for mechanical inspiration. Initially we designed our turbine with a similar egg-shaped outer shell, rear fin, and helicopter-like blade pitch system. After months of design work and consideration, we decided to stop developing our own pitch control system and began work on a less sophisticated but more robust way to modulate RPM using our mechanical brake system. The egg-shaped outer shell changed shape over time to accommodate our driveline assembly and quickly became our own. The rear fin design process was similar. We began with a large split wedge inspired by the Wild Cat's design. After initial testing, it was determined that the fin had to have a larger surface area to counteract the weight of our turbine, so we adapted this design so that our turbine could turn more effectively at lower wind speeds.

We also chose our generators in a similar way. Our original choice was the MAD 5015 motor, which is similar to the motor chosen by Northern Arizona University. However, we later changed our motor choice to the Antigravity MN6007, which was one of the motors tested by John Hopkins.

The team began the blade design process very different compared to some teams. Being influenced from the shape of a maple tree seed, the first set of blades had a nonlinear distribution and most of the surface area farther from the hub. Maple tree seeds were naturally good at autorotation, so we assumed this would applicable to rotation on a horizontal axis wind turbine. Once QBlade was found as a beneficial software, our team used the blade optimization function which resulted in a design less like the maple tree seed and more similar to blades from other teams in previous competitions.

Mechanical Systems

Static Performance Analysis

The graph depicted in Figure 1 is a way to compare different blade designs by looking at their power coefficients at varying tip speed ratios. The tip speed ratio (TSR) is a ratio of the incoming wind velocity to the rotational speed of the blade tip. To prioritize the power generation section of testing, our design was made for wind speeds between 5 and 11 m/s. Although the blades will be durable up to 22 m/s, this was given less consideration regarding power output. The light blue

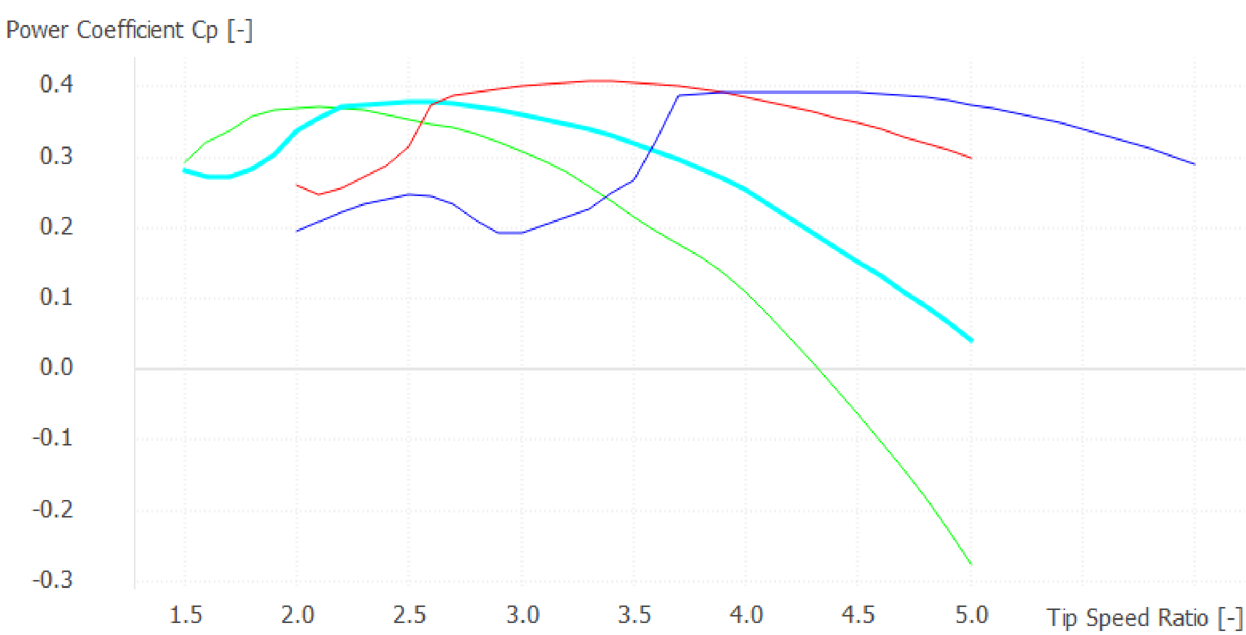

Figure 1. Coefficient of Power vs Tip Speed Ratio

In Appendix A of the Rules and Requirements for the Collegiate Wind Competition, there is a slightly higher weighting for power output at 5 – 8 m/s as opposed to 9 – 11 m/s. The power curve performance test focuses on highest wattage production, but the control of rated power test implements a varying load to obtain a constant power throughout the windspeed range. Essentially, we are focusing on keeping the r_p value as close to 1.000 as possible, to follow the rules. To accomplish this, optimization on the blades was done for 6 m/s windspeed.

Mechanical Systems

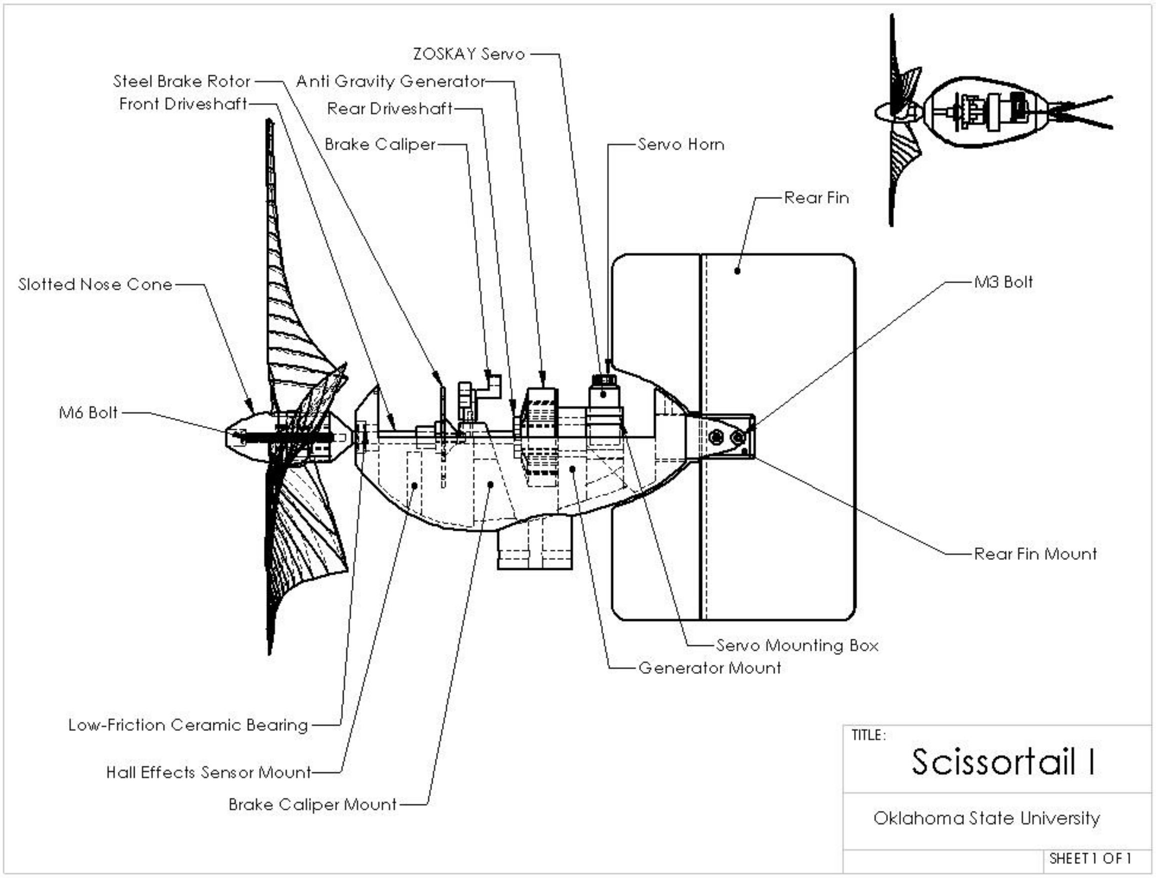

Figure 2. Mechanical Schematic

Blade Design

In the beginning of the blade design process, preliminary analysis was performed with MATLAB. Blade Element Moment Theory (BEMT) is a type of code intended to analyze the performance of turbine blades at certain rotational speeds and varying tip speed ratios. However, because of the nonuniform nature of the blade profile the original MATLAB code was insufficient for the team's tasks. QBlade was utilized in order to include the nonlinear distribution that the team was trying to design.

In this new software, the team was able to choose an airfoil and insert it into the program. The SG6042 airfoil was chosen because of its high lift-to-drag ratio, so we used this airfoil for the entire length of the blade. In compliance with the rules of the competition, the longest length that blades could be was 20cm, after considering the size of the nosecone. Power from the wind is dependent on the area of the blades, so we decided to maximize the length and set it as a constant in the design process. The dimensions we chose to adjust next were chord length, twist, and pitch. Part of QBlade's program allows for optimization of chords and twists. To optimize twist, one must insert the angle of attack at which the optimal lift-to-drag ratio occurs. We tested a set of blades that had a TSR of 2.2 and a cut in speed of 4 m/s, while another set of blades with a TSR of 3 had a cut in speed after 5 m/s, which is unusable given the competition's specifications. Power generation tests for the span between 5 and 11 m/s so the cut in speed needs to be as low as possible. Lower tip speed ratios correspond to larger blade areas, but those designs are still very capable of reaching rotational speeds exceeding 3000 RPM. Based on these findings from our initial wind tunnel tests, we chose TSR of 2.5.

We chose to use PLA for the material of the initial versions of the blades. The final design is 3D printed using a Markforged Onyx printer that can run a strand of carbon fiber through the middle of the PLA to reinforce the blades. This carbon fiber reinforcement will have material properties and strength like that of aluminum while maintaining a lightweight structure.

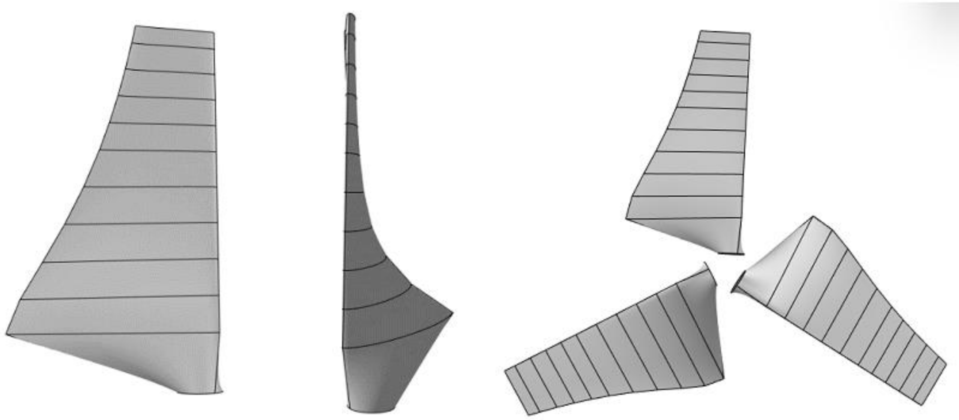

Figure 3. QBlade Blade Design

Blade Testing

To test our blade designs, we connected our blades to a motor in a wind tunnel. This motor was an RC plane electric motor, which was connected to a LabVIEW data acquisition system that noted RPM from a hall effects sensor built into the motor. For each test we subjected the blades to wind speeds up to 16 m/s since it was the highest wind speed at which we could obtain accurate data. The objective of our tests was to evaluate cut-in speeds and max RPMs to continue to optimize our blades to choose a final design. We performed 6 tests, each with a different blade design. From the first three tests we concluded that the blades designed with higher pitch and a larger surface area achieved the best results. Therefore, new blades were designed and tested.

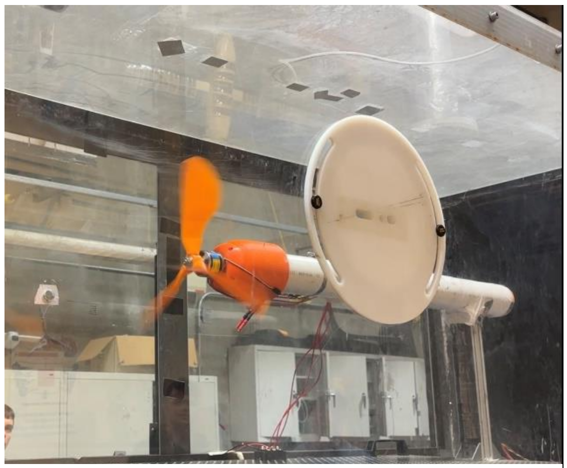

Figure 4. RPM Blade Testing

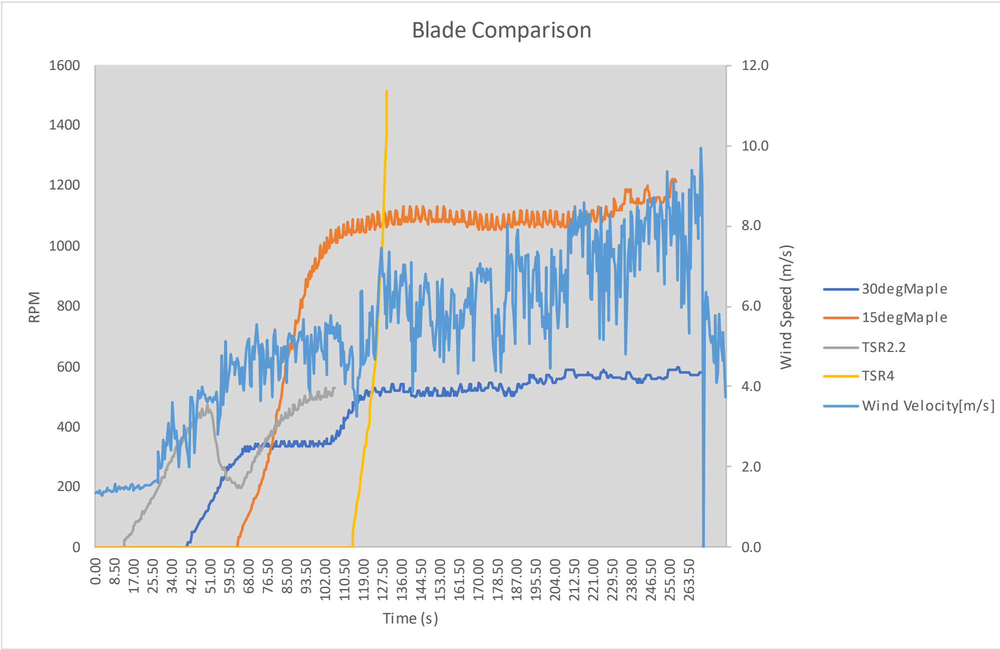

Figure 5. Blade testing in the wind tunnel

As shown in Figure 5, there were two blades that had desirable outputs, which were blades with TSRs of 2.2 and 4. The TSR of 4 produced 1500 RPM, but not until 8 m/s, whereas the TSR of 2.2 produced an RPM of only 500 RPM with an earlier cut in speed of 3.8 m/s. Therefore, a hybrid design of the two TSRs was produced.

We performed two types of stress tests, the first being a stress test for our blades in the whole nacelle system. We wanted to see if our blades could withstand the torque produced from the driveline spinning at high RPMs. To perform this test, we assembled our nacelle system on a base and connected a battery load. The maximum rpm our system withstood was 3300 for two minutes. The second stress test was focused solely on the forces the blades could withhold. Blades were placed in a vice, then weights were attached at the tips of the blades with increased mass until failure. The blades failed at 3 kg which is a force of 29 Newtons. This was done with PLA 3D printed blades, however, our final blades are printed with carbon fiber reinforcement which will cause the blades to be stronger, but more brittle.

Driveline System

The driveline was designed to meet two major requirements: transfer energy from the blade assembly to the generator as efficiently as possible and provide a mount for the floating brake rotor.

To connect the blades to the driveline, a nose cone was needed. The nose cone was designed with three offset slots to align the blades to the same plane of rotation. Each slot has a flat area where the blades rest to help prevent bending of the tabs. For the mounting, the nose cone has a square hole on the back where the front of the driveshaft is inserted. This was to establish that the nose cone would not spin independently from the driveshaft. The nose cone was designed with a recessed hole for a 6 mm bolt to fasten the nose cone through the blades to the driveshaft. It was 3D printed using PLA, as shown in Figure 6.

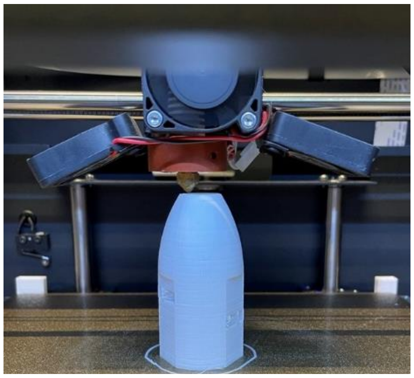

Figure 6. Nose Cone

As stated in our previous report the driveline experienced rotational bending at the joint during testing, which led to a redesign. The two-piece design was kept, but a collar was added to the rear (female shaft of the driveline). The front male shaft is supported by the front bearing and has a threaded stud that screws into the rear female side of the driveline. The outer diameter of the male side is dimensioned to fit with a concentric interference fit into the collar of the rear driveline that encapsulates the female threads and secures the two halves together. The rear shaft is mounted to the brushless motor and the driveline can be easily split to aid in assembly/disassembly. The addition of this collar in tandem with a material change to CNC aluminum provides the bending strength the driveline was lacking. Both the male and female drive shafts were manufactured using a CNC lathe and a 5-axis CNC mill. The symmetrical circular geometry of the driveline was lathed out of 6061 aluminum stock. The non-circular geometry and holes were manufactured via either the CNC 5-axis mill or a manual mill. Threads and taps were done manually.

Figure 7. Driveline manufacturing

Friction and rotational inertia have been decreased to provide the lowest torque to cut in and operate possible. The driveline was resized to allow for a high-speed ceramic bearing greatly decreasing the required rotational torque. The previous brushless motor was also replaced with a low-cogging torque equivalent that reduces cogging torque by 250%. Rotational weight has been reduced by decreasing the diameter of the front and rear shafts and decreasing the size of the lofts between mounts.

The brake rotor used required the driveline to be two pieces because the rotor had to be able to be secured in the middle of the driveline. The solution for this was the two-shaft design allowing the rotor to mount onto the rear shaft and the front shaft threaded into the rear.

Braking System

The braking system takes advantage of two braking subsystems: the brake force created by the motor and the more abrupt force created by the mechanical disc brake. This system was designed to work in tandem with the hall effect sensor and the electrical system. The sensor will sense the RPM of the driveline and vary the applied brake force to stay as close to an r_p of one as possible to maximize our points.

The motor braking system is designed to finely aid in RPM modulation. The brake force of the motor is varied using the load's resistor which allows for more precise braking compared to the mechanical brake.

The mechanical brake is used to quickly reduce RPM, park, and restart. The mechanical brake has much less modulation than the motor braking system but has a much larger brake bite and stopping torque. The mechanical brake is modulated using a servo and linkage system which was revision. The servo was chosen for its quick actuation speed of 0.12 seconds per 60 degrees at 5 V. This servo will be powered by 5.5 V which will ensure sufficient actuation quickness.

Brake Testing

For an initial test, we wanted to see if the braking system would be able to modulate RPM and stop the turbine. To perform this test, we attached a drill to the driveline that subjected the driveline to an RPM of 2000. A lab bench power supply and pulse generator controlled the servo to engage the mechanical brake. The servo successfully employed the brakes and could modulate the RPM, so the final brake test was performed to completely stop the system.

A second brake test was performed using parameters similar to the competition in a wind tunnel. The complete nacelle system was installed in a wind tunnel which subjected the turbine to wind speeds up to 22 m/s. The PCC wires were connected to a 7.5 Ω resistor which helped keep the RPM at 100. The load can create a lower resistance to increase the power draw and therefore slow the RPM even more. This test verified that the load is sufficient for regulating the RPM.

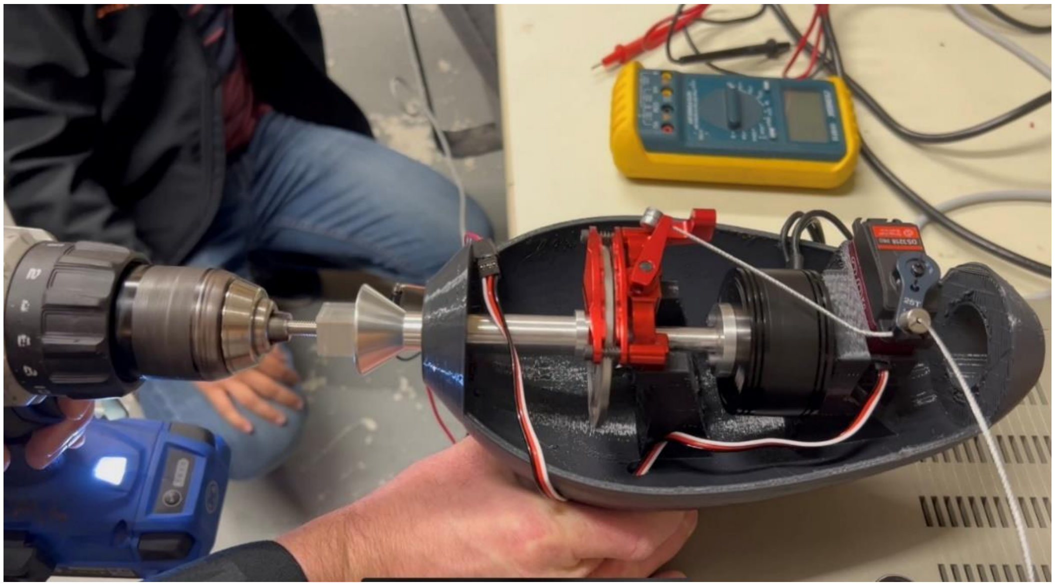

Figure 8. Testing the performance of the mechanical brake

Yaw System

We designed the yaw system to be lightweight, while still providing enough surface area for fast and effective rotation. The twin-fin design was selected to reduce wavering of the system. The initial design for the fin did not work as hoped when tested with a fan, so the design was altered to provide a larger surface area while staying within the size constraints given. The larger surface area of the passive yaw system resulted in the turbine turning into the direction of the wind as desired. All prototypes were 3-D printed with PLA, but the final design was made from acrylic due to ease of fabrication and sizing constraints with 3-D printing. Because the yaw was so easy to manufacture and assemble, this also allowed for more efficient testing.

Yaw Testing

To ensure the nacelle will adjust to wind direction at competition, the yaw system was tested physically and through simulations. In the design phase, CFD was used to determine the effects (pressure/stress) of wind coming from different angles. This determined the angle we needed was 15 degrees for each fin to be offset to successfully align the nacelle toward the wind. To physically test, we measured the wind speed of an oscillating fan using an anemometer, which measured a wind speed of 4 m/s. We determined that because the yaw could adjust successfully at a low wind speed, it would adjust at higher wind speeds.

Figure 9. Yaw Subassembly

Nacelle Design

The Nacelle was designed to provide support and be a mounting point for the driveline, braking, and yaw subassemblies without failing or flexing during operation. Aerodynamic analysis was performed to aid in the design to reduce drag while encapsulating the assembly.

Sturdy support and mounting for the driveline are crucial to the turbine's operation. During early testing the nacelle experienced flexion as the driveline rotated. We resolved this flexion by increasing the wall thickness of the nacelle from two millimeters to three millimeters and increasing the density of the 3D print. We also improved the mounting by adding structural webbing to the brake caliper mount and the brushless motor mount and setting the print to layer perpendicular to the incoming driveline force to further reduce bending during operation or heavy RPM modulation. The addition of a rear mount for the yaw control also aided in the nacelle's longitudinal stiffness.

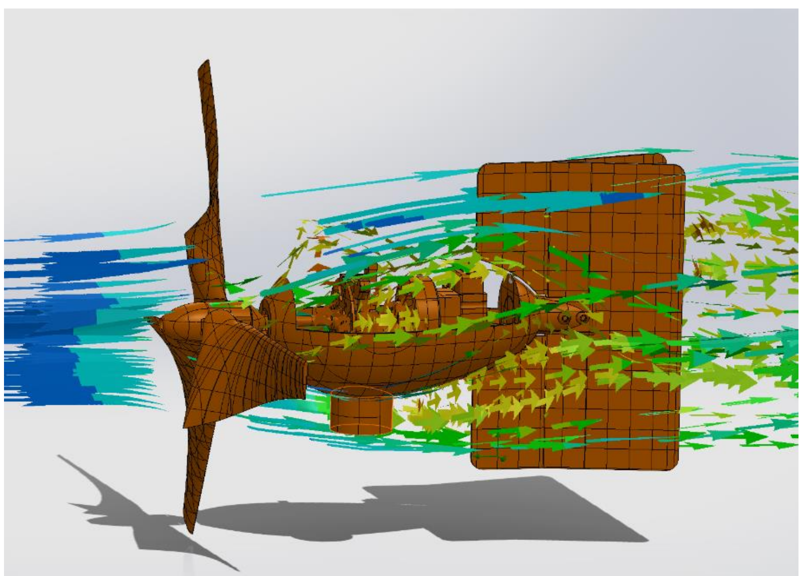

Figure 10. CFD of Nacelle Assembly

To reduce drag, the nacelle was made in the shape of a tear drop, which was inspired by previous teams. This tear drop shape is made up of four main concentric circles and lofts between each circle. The size of each circle is reduced as much as possible to contain the necessary components, while reducing surface area affected by the wind. By decreasing the surface area, we minimized the profile drag.

Simulations, as well as physical tests, were also done to visualize wake effects over the nacelle and tail after the turbine blades were subjected to wind.

Connector Design

A connector was necessary to attach the yaw to the rear of the nacelle and ensure the system stayed in place. This piece connects to the nacelle with a bolt that goes through the top to hold it in place. The fins are then attached to the connector with 2 bolts each so that the pieces are all secure in the wind tunnel. The connector ensures that the two fin pieces stay 15 degrees apart and was fabricated with PLA using 3-D printing.

Foundation

Engineering Diagram

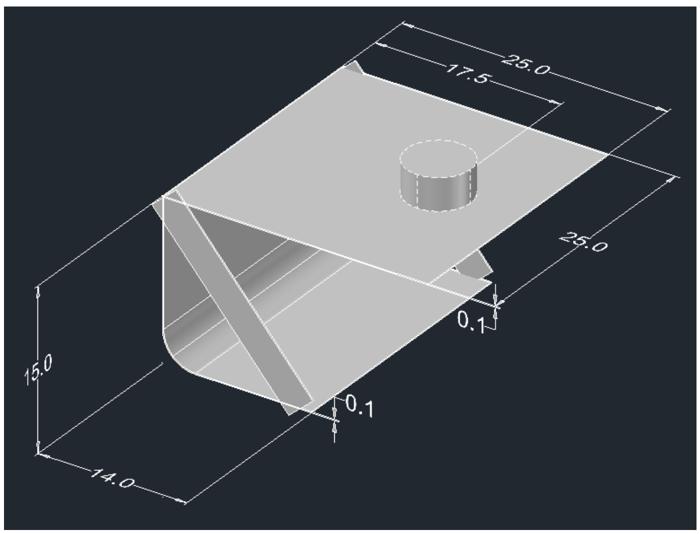

Figure 11. Foundation Design (Measurements in Centimeters)

Structural Analysis of Foundation/Anchoring System

The competition rules are very clear about the testing conditions of the turbine, making data collection for moment calculations relatively easy. Our turbine needs to be able to withstand a maximum wind speed of 22 m/s. To convert this wind speed into a distributed load across the turbine structure and to calculate the drag created by the turbine blades, the density of air needed to be found. It can be assumed that the air within the wind tunnel will be at standard conditions for Boulder, Colorado, so the air density used is 1.14 kg/m^3. The soil used in testing is Lowe's item number #293326 which is a uniformly graded fine sand. Knowing this, the density and the porosity of the sand can be found. The density of the sand is 1.631 g/cm^3 and the porosity is 0.29. The sand used for testing will also be saturated in water, leaving little-to-no air voids. This means it can be assumed that all the voids in the soil and water mixture are filled with water. All this information was beneficial in our design process.

Before designs were made, CFD analysis was conducted to determine the maximum moment the foundation would need to withstand. By running this analysis, we determined that the turbine would need to resist about a 7.2 lb-ft moment.

The rules state that the turbine can only move 2.5 cm during testing, which means the design must withstand the moment of the wind load applied to prevent tipping. The rules also state that when we install the turbine for testing, we cannot touch the water or sand with any part of our bodies. The anchor must not exceed more than 20 cm of sand penetration and the foundation must be able to be installed within the 25-minute time limit given.

To calculate the moment the foundation design could withstand, we found the volume of sand and water mixture that would be resisting the rotation of the foundation. Using this volume of the mixture, we found the volume of the voids by multiplying the total volume by the porosity of fine sand, as shown in the equation below.

$$V_{voids} = nV_{total}$$

The volume of the voids can be assumed to be the volume of the water in the mixture because the sand will be completely saturated during testing. To find the volume of sand, we subtracted the volume of water in the mixture from the total volume.

$$V_{sand} = V_{total} - V_{voids}$$

To find the total mass of the mixture, we multiplied the density of water (1 g/cm^3) by the volume of water and then added to the density of the sand multiplied by the volume of the sand.

$$m_{mix} = V_{sand}\rho_{sand} + V_{water}\rho_{water}$$

Next, the mixture's weight was found by multiplying the mass by the gravitational constant acceleration on earth (9.81m/s2).

$$W_{mix} = m_{mix}g$$

We found the moment by multiplying the weight of the mixture by the approximate centroid of the shape, where the force would be located. This value was then added to the weight of the turbine multiplied by the distance its centroid is from the tipping point.

$$M = W_{mix}d_{mix} + W_{turbine}d_{turbine}$$

The foundation selected was a scoop design with two trusses on either side and a truss down the middle. After creating the design in AutoCAD, the anchor was fabricated and tested. The final weight was ~1869 grams and could withstand a moment of 12 lb-ft. The foundation was made to be easily installed by one or two people. The anchor will be installed by scooping into the sand as deep as possible without touching the water on top of the sand and then using a concrete vibrator to fully set it into place. Once installed into the sand it is ready to be used.

The anchor was fabricated out of steel by MIG welding.

Anchor Testing

To test our anchor, we began by installing our anchor into our sandbox in alignment with the competition rules to model how our anchor will act at the competition. We then used a force scale to pull the top of the anchor from multiple angles, simulating different angles of wind, to dislodge the anchor. We then recorded the force values in Newtons that caused the anchor to become unstable and multiplied them by the length, in meters, from the base of the anchor to the top, to determine the maximum moment our anchor could withstand before failure. We found that our anchor was more than capable of withstanding the expected moment of the wind.

Electrical Systems

System Overview

Figure 12 shows a one-line diagram of the electrical system. The electrical system is split into "Turbine Side" and "Load Side," as shown. Both sides have a Teensy 4.1 microcontroller. The turbine-side microcontroller (TCPU) detects RPM using a hall effect sensor, calculates power generation, and controls the servo for the brake. The load-side microcontroller (LCPU) controls the resistor bank and the power back-feed system for when the turbine is stopped.

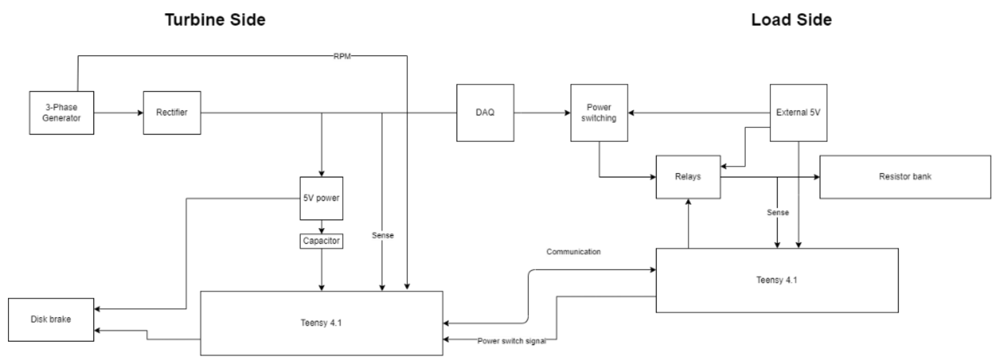

Figure 12. One-line diagram of the electrical system

Generator

We decided that the generator should be a three-phase brushless motor with a kV of around 100 to 200. Three-phase brushless motors are inherently more efficient and have less overall friction, even though a rectifier will be required to convert the output to DC. A kV between 100 to 200 would produce enough voltage to increase the efficiency of the power transmission through the lines. It is also easier to step down voltages than to boost voltages, which will make it easier to power the onboard electronics at lower RPMs while the turbine is starting up. This range of kV is also high enough to avoid going over the 48 V limit since the turbine's theoretical absolute maximum RPM is about 3000 during a catastrophic brake failure, which would produce 30 V from a 100 kV motor.

The generator was originally chosen to be a MAD 5015 150 kV brushless drone motor. However, through testing, it was discovered that the cogging torque of this generator was higher than expected. Therefore, this generator was replaced by an Antigravity MN6007 160 kV brushless motor that advertised a low cogging torque. The cogging torque of this new motor was confirmed to be about 2.5 times less than the MAD motor.

Generator Testing

We tested the generator by connecting a drill to the driveline that is attached to the generator, and the generator output was connected to a rectifier and a 470 µF capacitor. The drill had two speed settings being 500 and 1750 RPM; we tested the generator at each RPM value in three trials of 30 seconds each to get an average voltage produced at both RPMs. We concluded that our generator was only capable of producing 2.2 V at 500 RPM, which was much too low, leading to a focus on increasing the RPM of the blades.

Buck Boost Converter

Power from the generator can be used by the Teensy 4.1 microcontroller through the use of a buck boost converter circuit. Voltage is passed from the generator to the input of the converter circuit, which can take voltage ranging from 2.7 V to 40 V, which is more than enough to cover any amount the circuit would receive from the generator. The circuit converts the input voltage to the 5.5 V required for the Teensy 4.1 and servo motor to function, stepping up the input voltage if it is less than 5.5 V and stepping down the voltage if it is greater than 5.5 V. The circuit, pictured below in Figure 13, consists of the converter itself, along with several surrounding components serving various purposes such as regulating the frequency of operation, avoiding output oscillation, and defining output voltage using a voltage divider.

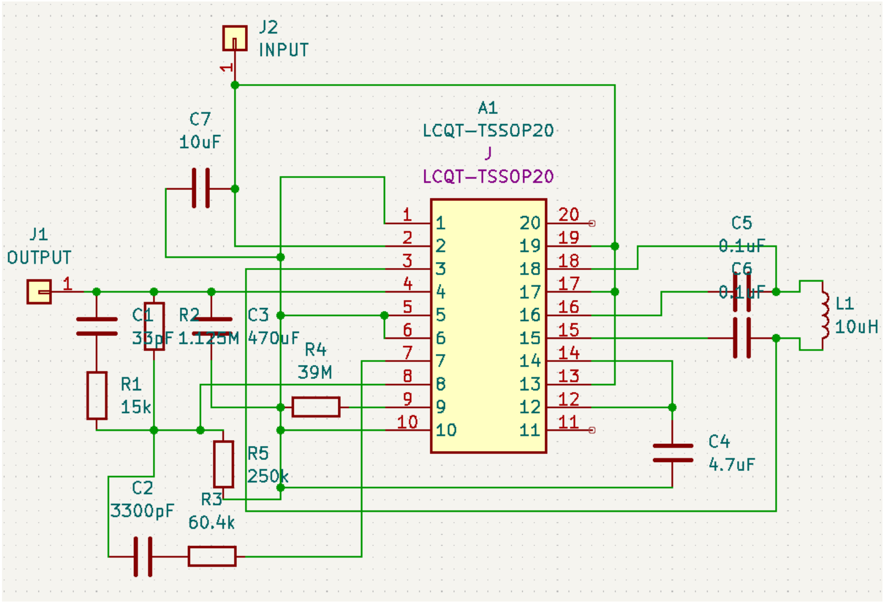

Figure 13. Buck Boost converter circuit

The circuit was assembled on a PCB and installed inside the nacelle of the turbine. Power travels from the generator and rectifier into the circuit, and after going through the circuit and being stepped up or down, is passed to both the Teensy microcontroller as well as the servo used for braking.

Load System

The load system is designed as a controllable resistor array that self-adjusts its resistance value based on input power and voltage calculations. As shown in Figure 14, the total resistance is altered with the use of IRF510N MOSFETs driven by the LCPU, with non-inverting amplifiers used to drive the voltage output of the LCPU up to 10 V, which is the gate voltage required to pass the expected current generated from the turbine. For each transistor's gate that is activated, the current will bypass the resistor connected between its drain and source and move through the rest of the load.

Our software model is built to step through each resistor, providing a range of values from 7.5 to 165 Ω. Using a 5 V relay and a control signal from the LCPU, our load system can switch from receiving to back-feeding power to power the TCPU and Servo during startup and controlled shutdown.

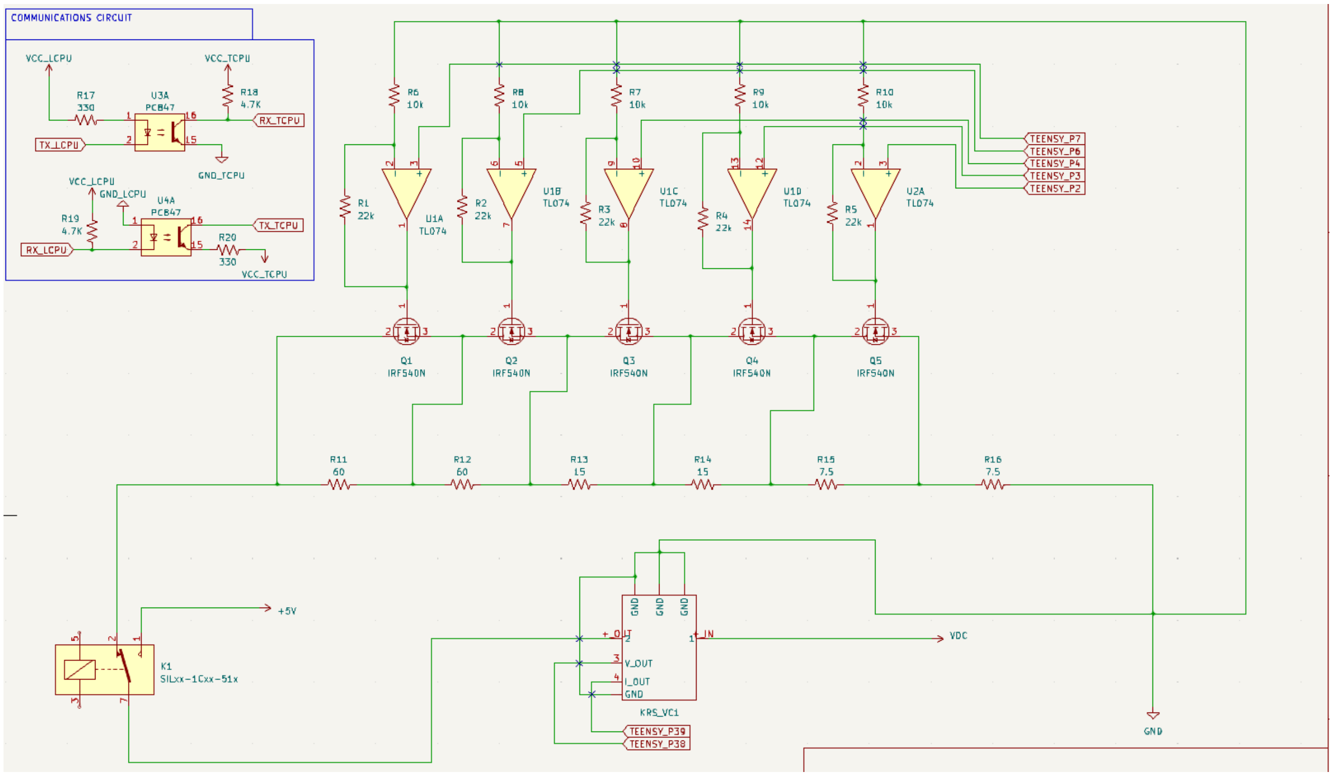

Figure 14. Load-side Schematic

Control Model Analysis

The electrical system operates in three different modes of control: Start-up, generation, and shutdown.

In start-up conditions, power is back-fed to the turbine until a threshold RPM is reached from wind power generation, at which point a flag is sent to the LCPU to stop the back-feed and begin load control, leading to generation mode. Generation mode works as described in the above sections — the TCPU monitors RPM conditions and controls the buck-boost converter while the load adapts to control RPM and sink the power generated from the turbine.

There are two kinds of shutdown: controlled and immediate. In controlled shutdown, resistance is set to the minimum value of 7.5 Ω, with the load acting as a brake to slow the turbine down. Once RPMs are below the threshold value, power is then fed to the TCPU. In immediate shutdown, triggered by the competition's shutdown button or load disconnection, a signal is sent from the LCPU to the TCPU to trigger the mechanical brake, which will be operated on the residual power generated from the turbine before it stops.

Software Architecture

All software is executed on turbine and load-side Teensy 4.1 microcontrollers using C code. On the turbine side, RPM is measured by counting the number of times the hall effect sensor detects the magnet installed in the rotating driveline. This is then sent to both Teensy modules, and RPM is controlled via the load, described in more detail below. In the event of a shutdown, the code commands the servo closed using remaining power so that the blades will not rotate even when the load is unavailable to control the RPM.

On the load side, conditions relating to power are monitored with a KR-Sense 45A voltage and current sensor and RPM values received from the TCPU. Depending on the value of the power output, the resistor array is set to most aptly control the speed of the turbine and prevent surges. The LCPU also handles flags relating to braking and shutdown protocol depending on the power being received from the turbine, in addition to triggering the 5 V back-feed that powers the TCPU and brake servo in startup and controlled shutdown.

Since power is only allowed to be transferred through the competition-provided PCC cables, communication between TCPU and LCPU is handled through UART communication. UART communication is done through optically isolated communication lines to ensure no power is transferred between the turbine and load side of the system.

Final Assembly

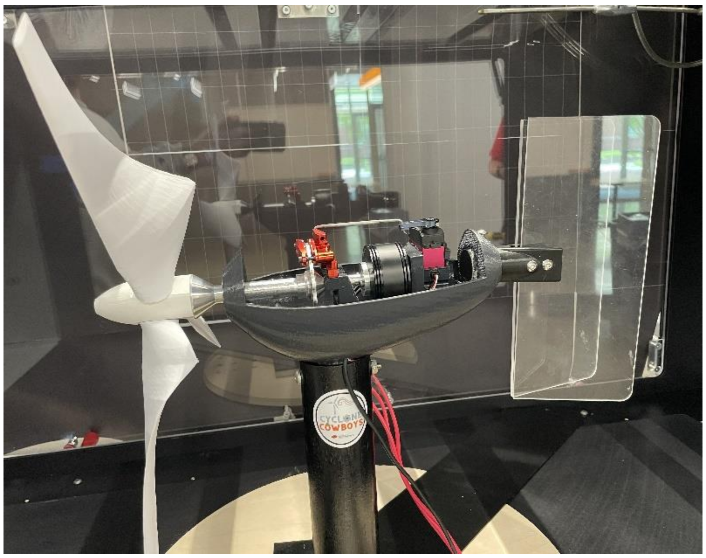

Figure 15. Assembly of Subsystems within Nacelle

Final Assembly of Subsystems

After we designed and fabricated the individual subsystems, we integrated them into the final assembly. We designed the blades with 7.5 mm (about 0.3 in) rectangular tabs to fit into offset slots in the nose cone. This allows the blades to turn on the same plane of rotation. The nose cone, blades, and rear fin are secured with an M6 bolt threaded onto the nacelle assembly. The nacelle is set in a milled aluminum “turret” that is welded to the 52 mm bearing on the top of the post. Designed with the CWC-provided stub in mind, the post and nacelle assembly can be connected for competition testing. The anchor was fabricated out of steel and MIG welded to a foundational post. All subsystems are designed and assembled to be effective in the dimension constraints set by the CWC. All sub-teams communicated efficiently and relied on one another to bring each subsystem together into the final assembly.

Assembly/Commissioning Checklist

Before turbine is placed in wind tunnel

- Attach the tail piece to the nacelle with the 6 mm bolt.
- Make sure the front driveshaft is tightened into the rear driveshaft tightly with blue Loctite to make sure it does not come apart during testing.
- Spin blades to see if the rotor catches. If the rotor catches, loosen caliper mounting bolds and slide the caliper to appropriate position.
- Retry spin test. If it fails, adjust the brake pad clearance to where it is in line with the edge of the floating rotor mount on the driveshaft. Retest.
- Place nacelle base in turret bearing. Fasten to turret bearing.
- Make sure the “turret” bearing spins freely with nacelle attached.
- Turn on teensy to control the brake caliper servo. Test braking function

- Test load side for power generation readings.

Anchor Installation

- Attach CWC provided stub to anchor by tightening the bolts around the stub on the anchor.
- Install the anchor by driving the scoop opening into the sand.
- Place concrete vibrator onto middle of top plate
- Turn on vibrator until sand looks visibly settled.
- Measure distance from bottom of anchor to top of sand to ensure it does not exceed 20 cm.
- Verify that tubing is placed within 10 cm of CWC specified circle. Adjust if necessary.
- Use CWC given level to level the anchor in the sand.
- Run electrical cables through top tube of foundation.

Commissioning

- Run wind tunnel at varying speeds from 5-11 m/s to check shutdown.
- Once shutdown is completed with wind tunnel on check restart of turbine
- Measure power output.
- Shutdown wind tunnel.
- Measure anchor displacement and ensure it does not exceed 25 mm.